J Mol Model (2006) 12: 713–721
DOI 10.1007/s00894-005-0040-8

ORIGINAL PAPER

Oliver Weingart · Igor Schapiro · Volker Buss

Bond torsion affects the product distribution in the photoreaction of retinal model chromophores

Received: 23 May 2005 / Accepted: 26 July 2005 / Published online: 10 November 2005

Abstract Ab initio molecular dynamics (MD) calculations have been performed to study the photoisomerization of a 3-double-bond retinal model chromophore, the all-*trans*-4, 6-dimethylpenta-3, 5-dieniminium cation, and the possible influence of non-planar distortions on the product distribution. In total, 171 trajectories have been generated for four different conformations of the structure, a planar one and three in which the C4–C5 and the C5 = C6 bonds were increasingly twisted out of plane. Starting geometries randomly distributed about the equilibrium geometry were generated by zero-point energy sampling; trajectories were calculated using CASSCF-BOMD methodology and were followed until the photoproduct and its configuration could be assigned. For the latter, two different approaches were applied, one involving the CASSCF configuration vectors, the other an analysis of the MD at the first possible hopping event. Isomerization was found to occur almost exclusively about the central C3 = C4 double bond in the case of the planar model compound. Twisting the conjugated π-system shifts the isomerization site from the central double bond to the terminal C5 = C6 double bond. With both the C4–C5 and the C5 = C6 bonds twisted by 20°, about 35% of the trajectories lead to the configurationally inverted 5-*cis* product. The results are discussed with reference to the highly selective and efficient photo-induced isomerization of the retinal chromophore in rhodopsin.

Keywords CASSCF · Molecular dynamics · Rhodopsin · Retinal · Isomerization

Dedicated to Professor Dr. Paul von Ragué Schleyer on the occasion of his 75th birthday.

O. Weingart · I. Schapiro · V. Buss (✉)
Department of Chemistry, University of Duisburg-Essen,
Campus Duisburg, 47048 Duisburg, Germany
E-mail: theobuss@uni-duisburg.de
Tel.: +49-203-3793315
Fax: +49-203-3792772

Abbreviations MD: Molecular dynamics · BOMD: Born–Oppenheimer molecular dynamics · ZPES: Zero-point energy sampling · Rho: Rhodopsin · bR: Bacteriorhodopsin · Batho: Bathorhodopsin · pSb: Protonated Schiff base · SA: State-averaged · CASSCF: Complete active space self consistent field · MCSCF: Multiconfigurational SCF

Introduction

One of the most efficient photoconversions devised by nature is the reaction which initiates the process of vision in the rod cells of the vertebrate eye. Isomerization of 11-*cis*-retinal, the chromophore of the visual protein rhodopsin (rho), occurs ultra fast and is highly selective and effective: the first spectral evidence of the photoproduct is found after 200 fs; the single product is all-*trans*-retinal, and the quantum yield of the reaction is 0.67 [1]. After isomerization of the chromophore, the protein passes through a sequence of intermediates in which the configurational change of the chromophore is transferred stepwise into structural changes of the protein, until the active state is reached and the visual cascade is started [2]. A reaction of comparable efficiency initiates the photocycle of bacteriorhodopsin (bR), like rho, a retinal binding 7-helical membrane protein with, however, a different function: bR pumps protons from the cytoplasmatic to the extracellular side of the membrane. The chromophore of bR is all-*trans*-retinal, and the photoreaction causes isomerization from all-*trans*-to 13-*cis* [3]. In rho and in bR, the chromophores are covalently bound via protonated Schiff base (pSb) linkages to the ε-amino side chain of lysine residues, Lys296 and Lys216, respectively (Fig. 1) and are buried deep within the binding pockets of their respective proteins. Both configuration and conformation of the rho [4, 5] and of the bR chromophore [6, 7] have been verified with high-resolution X-ray crystallography.

The unsurpassed efficiency of the protein-bound retinal photoreaction has been studied in several theoretical

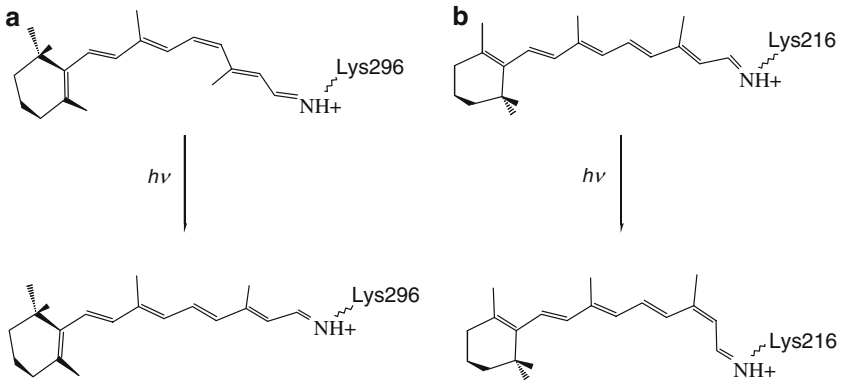

Fig. 1 The initial photoreaction of the rhodopsin chromophore from 11-*cis* to all-*trans* (**a**) and of the bacteriorhodopsin chromophore from all-*trans* to 13-*cis* (**b**)

investigations using either bare model chromophores [8–10] or chromophores within the binding pocket [11–13]. All studies agree that torsion about a particular bond is preceded by strong C–C bond vibration caused by the inverted π-electron density distribution along the conjugated chain in the S_1 excited state. Why bond torsion involves specifically the C11 = C12 bond in rho and the C13 = C14 bond in bR, is subject to considerable discussion. Undoubtedly, the protein pocket plays a major role, since outside the protein the photoisomerization of retinal pSb proceeds in a highly unselective and inefficient manner [14]. There are several distinct possibilities how the binding pocket might exert a directional influence on the photoreaction of the chromophore. Upon binding to the protein, the chromophore undergoes significant conformational changes resulting among other things in a pre-twist of the C11 = C12 and the C13 = C14 bonds. These torsions have been reproduced reliably with high-quality computations for rho [15] and for bR [16] and may be the prerequisite for the high stereoselectivity of the photoreaction. Also, the protein pocket is lined with charged and polar groups, which not only affect the absorbance of the chromophore but might also control the isomerization pathway by "electrostatic catalysis" [17]. Finally, and most difficult to prove or disprove by theoretical methods because of the computational effort involved, is the proposition that the excited chromophore induces transient structural changes in the protein that affect its chemical reactivity [18].

In this paper we show, on the basis of different 3-double-bond retinal model chromophores, that torsion, in particular the presence of pre-twisted double bonds, significantly affects the product distribution following photoisomerization. It appears that steric effects play an important role in the ultra fast and highly efficient reaction observed in the two proteins.

Computational details

Chromophore models

Ab initio molecular dynamics (MD) calculations are computationally highly demanding, which renders the treatment of the complete retinal chromophore impossible. We reduced the chromophore to a model consisting of the positive nitrogen center and the three adjoining conjugated double bonds (Scheme 1); the fragment from C1 to C9, which includes the β-ionone ring, was omitted and a methyl group introduced instead. For the numbering and the relation to retinal, see Scheme 1.

For this model, four different starting conformations were devised and geometry-optimized: **1** was kept planar throughout the optimization, in **2**, the C3 = C4–C5 = C6 and the C4–C5 = C6–C7 dihedral angles were twisted by 10° from planarity, in **3**, these angles were doubled, and finally in **4**, the dihedrals about the two bonds were taken from a realistic chromophore model obtained by

Scheme 1

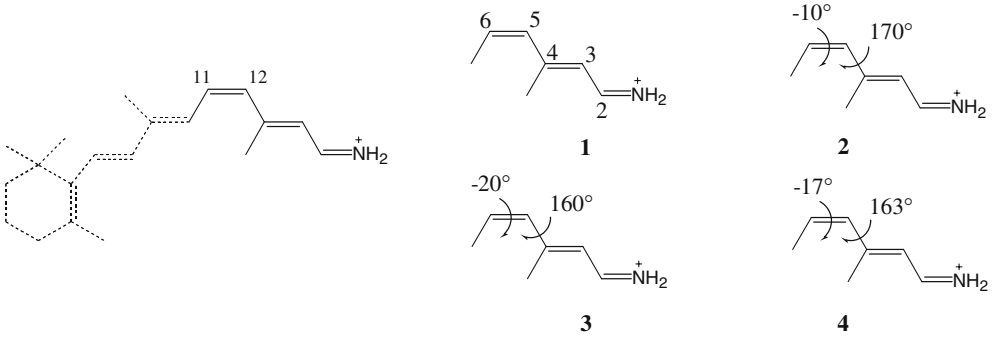

MD simulation of the complete retinal chromophore in the rho binding pocket [19]. Though the structures of models **2**–**4** do not correspond to local minima, their Hessians show no negative eigenvalues, since the molecules have not left the region of positive curvature of the torsion potential.

For the standard ab initio molecular orbital calculations, the GAUSSIAN98 program package was employed [20]. Ground state geometries were obtained by CASSCF optimization of the pure S_0 wave function using the standard 6–31G basis set and Cartesian *d*-functions. CASSCF configurations were formed by the six electrons in the six π-like orbitals of the molecule.

Trajectories

Excited-state MD simulations were performed using BOMD [21], which was adapted to the MOLCAS set of routines [22]. BOMD calculates trajectories on the excited S_1 potential energy surface by solving Newton's equations of motion on the fly using the Verlet integrator scheme with a constant time step of 0.24 fs. For the whole trajectory, state-averaged (SA) wavefunctions were employed with the ground and the first excited state weighed equally. SA-MCSCF gradients were corrected using Lagrange multipliers supplied by the MOLCAS-MCLR program. Velocities were scaled when the sum of potential and kinetic energy deviated by more than 0.06 kcal mol^{-1} per time step. Trajectories calculated this way reproduce exactly those obtained by the more accurate CPMCSCF gradient correction techniques [23] at significantly reduced computational expenditures.

For generating initial geometries and velocities for the MD calculations, the zero-point energy sampling (ZPES) method was employed. Described in detail elsewhere [24], second derivatives (frequencies) of the ground state CASSCF wavefunction are calculated, and zero-point energies apportioned to all vibrational modes. Potential and kinetic energy are distributed at random in the different modes, resulting in an ensemble of geometries that are identical in total energy but differ in their distribution about the equilibrium geometry.

Following Franck–Condon excitation from the S_0 ground state, trajectories are calculated on the S_1 surface. These trajectories eventually converge into the rotation of one particular double bond, with the S_1 surface dropping rapidly in energy and the S_0 surface increasing toward the region where surface crossing might occur. The most advanced method to determine the non-adiabatic surface hop event is by propagating the solutions of the time-dependent electronic Schrödinger equation together with nuclear propagation. After projecting the wavefunction on the adiabatic basis states, the population of the two states is used to determine whether a surface hop has occurred [25, 26].

Product formation

In order to avoid the accurate but very costly solution of the time-dependent Schrödinger equation, we have applied two alternative procedures to determine the fate of the trajectories. One is based on the "vector rotation" method and the other involves an analysis of certain torsional modes at the first possible point of decay. In the former, surface hopping is enforced when the scalar product of the CI-vectors of two consecutive MD steps indicates a change in electronic configuration [27]. The trajectory is then continued on the ground state surface, until the photoproduct (isomerization or return to the starting configuration) can be identified unambiguously. The vector rotation method can detect decay events only when there is a very close approach between the S_1 and the S_0 surfaces, and in most cases the molecule enters the crossing region several times before hopping is induced. In the following, we refer to these hopping attempts as "close approaches of S_1 and S_0." Typical energy differences for hopping events detected with this method are between 0.1 and 1.5 kcal mol^{-1}.

Surface hops, however, can occur earlier and at higher energy gaps. By solving the time-dependent Schrödinger equation, we have detected high probabilities of decay at the first close approach of S_1 and S_0 despite energy differences as high as 13 kcal mol^{-1} [28]. These results differ significantly from those obtained by vector rotation.

From the analysis of a large number of trajectories we have developed an empirical rule that allows to predict with high reliability the outcome of the photoreaction at any point of hopping, in particular at any point of close approach. The rule depends on the direction in which two dihedral angles about the rotating double bond are changing (Fig. 2): one is the torsion of the main chain measured as the dihedral angle C–C = C–C and the other is the torsion of the two substituents of this bond, i.e., the dihedral angle Me–C = C–H. In the case of C5 = C6 torsion, we have used the corresponding H–C = C–H torsion angle. Whenever the two dihedrals are changing in the same direction at the time of a possible hopping event, the product follows this direction. However, when the dihedrals follow different directions, it is the hydrogen with its strong out-of-plane movement that determines whether the S_0 trajectories will lead to the *cis* or to the *trans* product. At the point of first approach, these two angles are generally still in phase, and the probability of the *cis* product is high, if the molecule actually hops at this point. Later in the trajectory, especially after passing a point of close approach without hopping, the two angles uncouple and the probability of the *trans* product increases accordingly.

This torsion analysis method was applied at the point of closest approach of S_1 and S_0 (the point before both potentials start to diverge again) when the energy difference between the potentials at this point was less than 13 kcal mol^{-1}. It allows us to predict the fate of the molecule without the need to follow the ground state trajectory further. By applying this method to the

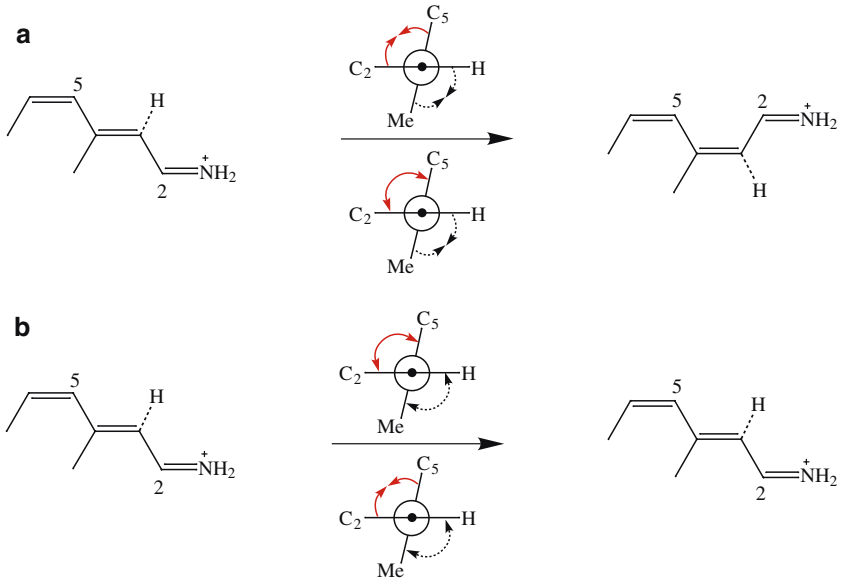

Fig. 2 Relationship between torsional modes and outcome of the photoisomerization. The reaction is productive only when at the decay point the H–C3 = C4–Me angle decreases, regardless of the C2–C3 = C4–C5 direction of motion (**a**). When this angle increases the starting configuration is regenerated (**b**)

cis-pentadieniminium cation, we were able to reproduce the product distribution obtained by time-dependent surface hopping exactly. It has also been used to determine the product distribution when starting from the *trans*-pentadieniminium cation [29]. It is the time-saving effect that has allowed the product analysis, i.e., the determination of the Z/E ratio, of the 171 MD runs of this study.

Results and discussion

In this section, we will first describe and discuss the features and general aspects of the calculated molecular trajectories. We will then present and compare the product distribution for chromophore **1** based on the two different methods for determining the hopping event. Finally, we will present the statistical analysis for all four chromophores.

"Productive" and "unproductive" photo-events

Figure 3 shows how several key molecular parameters evolve in time during a typical MD calculation. The left column of panels refers to a productive photoreaction in which one of the double bonds, C3 = C4 in this particular case, isomerizes from *trans* to *cis*. The right column

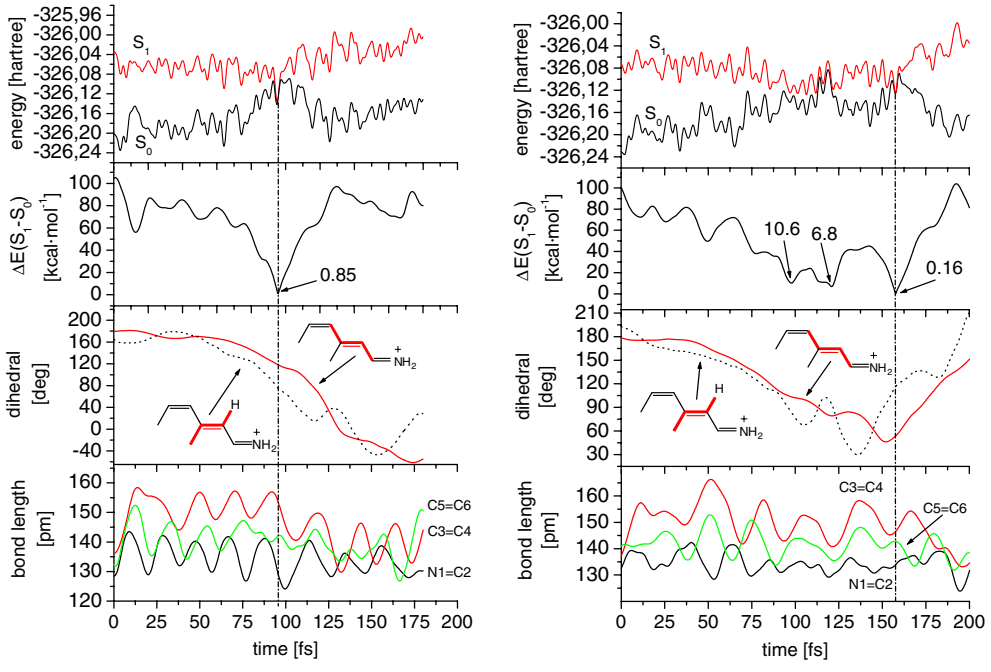

Fig. 3 Two trajectories of model **1**; *left*, trajectory that hops at the first close approach of S_1 and S_0 yielding the C3 = C4 *trans* product; *right*, trajectory that regenerates the starting configuration at the third approach of S_1 and S_0. The panels show (from *top*) the time development of the S_1 and S_0 energies; the energy difference, the C2–C3 = C4–C5 (*red full line*) and H–C3 = C4–Me (*dotted line*) torsion angles, and the double-bond lengths

shows how the parameters change in the case of an unproductive reaction, i.e., a bond starts to rotate, but at some point in time the rotation reverts and starting product is obtained.

The plots start with the Franck–Condon excitation from S_0 to S_1. The potential energy curves of both states show the high-frequency modulation caused by the fast C–H stretching vibrations. This is a result of the zero-energy sampling process in which all nuclei including the hydrogens have starting momenta and start to vibrate around their equilibrium positions. In the energy difference graph shown below, the C–H vibrational energy changes cancel out, in contrast to the energy changes due to the stretching modes of the double bonds, which are activated as a consequence of the electronic excitation. There is a conspicuous drop in the energy difference during the first 10 fs after excitation when all three double bonds start to adjust in-phase to the inverted electron density alternation of the S_1 state. This energy drop is singular since the vibrations start to dephase, which is obvious from an inspection of the bottom panel where the double-bond lengths are plotted against time. The strongest vibration is induced in the central double bond, which reaches a maximum length of close to 160 pm.

The third panel from top shows how the dihedral angles along the rotating bond changes along the trajectory. It reveals that the molecule is still essentially planar 60 fs after the excitation, when it slowly starts to rotate about the central bond. Concomittant with the rotation, the energy difference between S_1 and S_0 begins to drop sharply since the excited state is stabilized, and the ground state destabilized, by this torsional motion. After 95 fs, the energy difference has reached a value of less than 1 kcal mol^{-1} and the molecule hops back to the ground state. The continuing rotation carries the system quickly out of the hopping region, and the planar inverted geometry is reached after a total of 130 fs.

In the right trajectory, the molecule has already passed two close approaches—after 100 and 120 fs with energy differences of 10.6 and 6.8 kcal mol^{-1}, respectively, until it finally hops with an energy difference of 0.16 kcal mol^{-1} after 160 fs. The dihedral angle of the rotating bond is only 55° at the hopping event, i.e., the molecule has advanced significantly further toward the *cis* geometry than in the former trajectory, but this is not sufficient to realize a stable *cis*-configurated product. Instead, immediately after the hop the rotation of the bond reverts and the starting product is formed back. Note the rather smooth variation of the C2–C3 = C4–C5 dihedral angle in contrast to the erratic behaviour of the H–C3 = C4–Me torsion angle, especially in the neighborhood of close approaches of the energy curves. Also note that at the hopping event both angles are increasing again, allowing the prediction—as it turns out to be the case—that the product of this reaction will be the original all-*trans* configurated chromophore.

Product distribution: the vector rotation method

Forty-three trajectories were calculated and analyzed starting with the planar geometry of the chromophore model **1**. Despite the strain of the C5 = C6 bond due to the methyl groups at C4 and C6, there was only one trajectory in which this strain is released by torsion of this bond; 42 trajectories gave products resulting from C3 = C4 bond torsion. There is a broad distribution of hopping geometries, as shown in Fig. 4 (left). The Z/E ratio (i.e., productive vs. unproductive events) is large when the torsion angle is still large and hopping occurs at the first close approach. With decreasing torsion angle, the probability of unsuccessful approaches of the energy surfaces increases, and so does the fraction of unproductive events. In most of these cases, two or more approaches are necessary before the molecule actually decays. The calculated quantum yield is 0.6. Like the hopping geometries, the lifetimes of the excited states (Fig. 4, right) are spread out, and again there is a preference for high Z/E ratios when the lifetime is short.

Product distribution: hopping at the first close approach

Figure 5 shows what happens when the molecules are assumed to hop at the first close approach of the surfaces. Not unexpectedly the results differ substantially from those obtained with the vector rotation method,

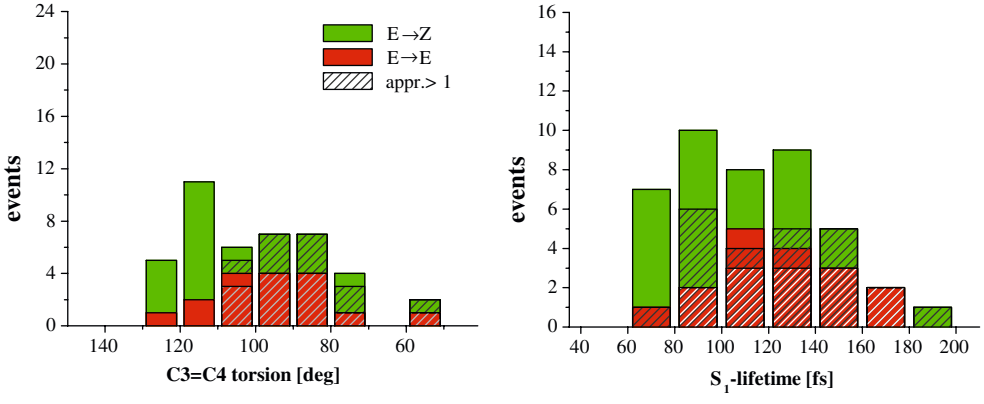

Fig. 4 Distribution of torsion angles at the hop point (*left*) and excited state lifetimes (*right*) for model **1** determined with the vector rotation method. *Lined boxes* denote trajectories not decaying at the first approach of S_1 and S_0

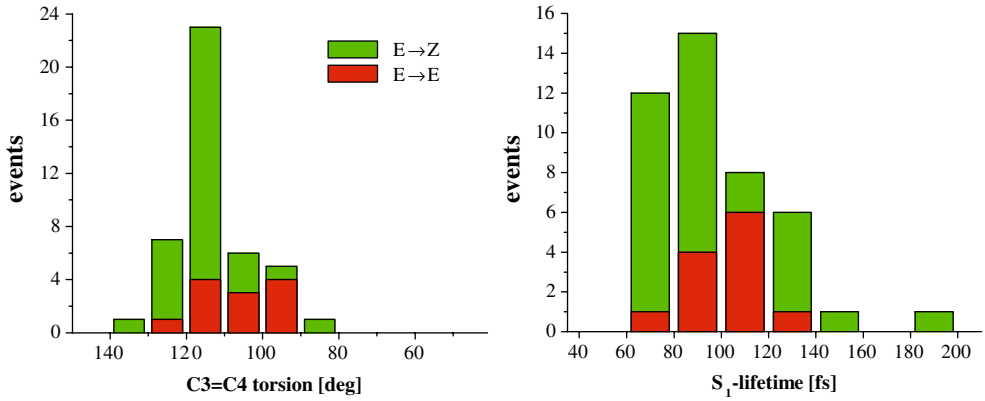

Fig. 5 *Left*, distribution of torsion angles and expected product distribution at the first close approach of S_1 and S_0 for model **1**; *right*, excited state lifetimes until the first close approach is reached

since the time that the molecules spend on the excited state surface is significantly reduced. One indication for this is the narrow distribution of torsion angles at the possible hopping event: since the molecules have less time for equilibration in the excited state, the hopping geometries are more similar. Fast decay is obviously connected with productive isomerization; more than 50% of the *cis* product is formed in less than 100 fs, while the majority of trajectories yielding starting material have lifetimes between 100 and 120 fs. In total, 30 out of 42 trajectories, i.e., 71% yield the *cis* product, compared to 60% when the vector rotation method is applied.

The two methods yield upper and lower bounds to the correct solution based on time-dependent quantum theory: the first possible event for surface hopping occurs when the surfaces approach sufficiently, whereas at a surface crossing the molecules will necessarily decay to the ground state.

The distribution of energy gaps (Fig. 6) is similar to that found in a non-adiabatic surface hopping MD of the *cis*-pentadieniminium cation [28, 29]. In nearly 60% of the trajectories we observe very small energy gaps of less than 4 kcal mol^{-1}, where surface hops are in fact highly probable.

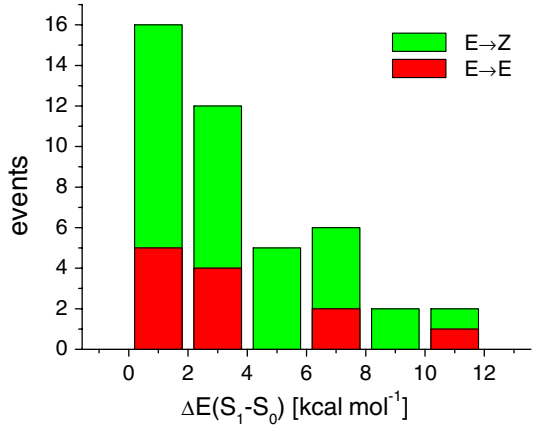

Fig. 6 Distribution of energy gaps at the first close approach of S_1 and S_0 for model system **1**

Effect of bond torsion on the product distribution

In total, 171 trajectories were calculated for the model chromophores **1**–**4** and analyzed with respect to the product distribution. The question which bond is going to isomerize can be answered very early in the trajectory as the rotatory motion is funneled into a particular site of the molecule. Whether the trajectory will yield the *Z*-product after hopping, or will reverse itself and return to the starting *E*-configuration, has been decided by an analysis of the chromophore dynamics at the first close approach of S_1 and S_0 as described in a preceding section. The results are summarized in Table 1, which also lists averaged values for the dihedral angles, the energy differences at the first close approach, and the time needed to arrive at this point.

Turning first to the question whether the non-planar distortion of the chromophore determines the position that is going to be affected by the photoreaction, we note that the fraction of molecules in which the central C3 = C4 bond isomerizes decreases significantly

Table 1 Summary of calculations for chromophore models **1**–**4** showing the total number of trajectories calculated and the number of C3 = C4 and C5 = C6 isomerization events

	1	2	3	4
Number of trajectories	43	44	43	41
C3 = C4 rotations	42	39	27	34
Productive	30	31	18	28
Clockwise	24	23	19	21
ϕ_{av}	114.3	112.2	109.6	114.0
ΔE_{av}	3.6	4.2	4.9	4.4
τ_{av}	98.4	96.3	99.7	93.6
C5 = C6 rotations	1	5	16	6
Productive	1	4	15	5
Clockwise	1	5	16	6
ϕ_{av}	80.2	82.5	80.3	92.2
ΔE_{av}	0.8	6.9	4.5	3.45
τ_{av}	114.7	83.0	81.8	87.7

For both types of isomerization, the table lists the number of productive runs yielding the *Z*-product; the number of trajectories following clockwise rotation; the average torsion angle ϕ (in degrees) of the rotating bond at the first close approach, the S_1-S_0 energy difference ΔE (in kcal mol^{-1}) at the first close approach and the excited state life time τ (in fs)

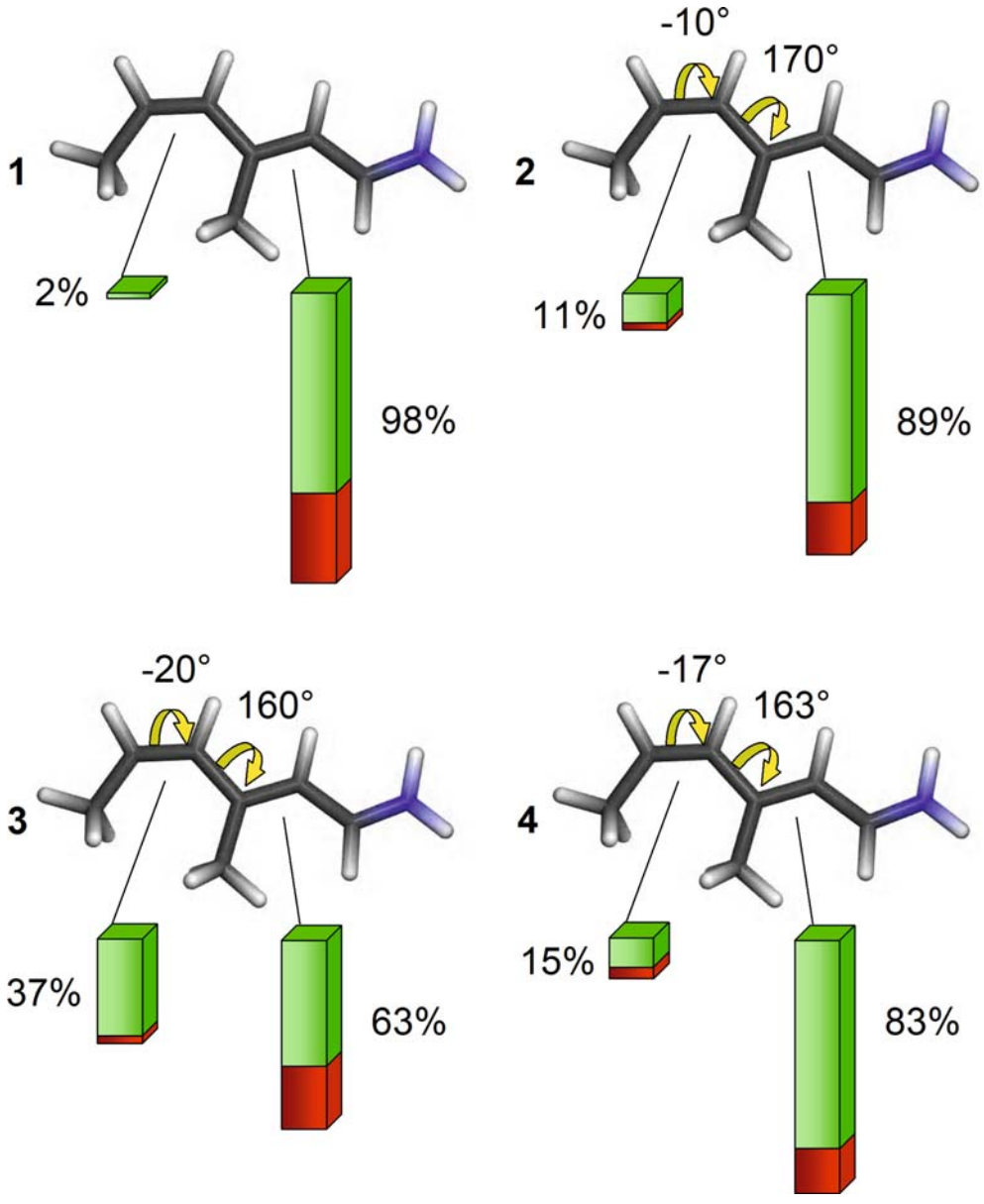

Fig. 7 Product distribution in the MD simulations of models **1**–**4**. The percentage of trajectories that lead to either C3 = C4 or C5 = C6 rotation is given beside the bar graphs. The *green* and the *red* portions of the bars represent, respectively, the productive and the unproductive events with respect to that particular rotation estimated from the torsion angles at the first close approach of the energy surfaces

as the twist of the two terminal bonds increases. The number of C3 = C4 isomerizations drops from 42 in the planar model **1** to 39 in **2** and finally to 27 in **3**, the model with the largest twist. In the same order the number of trajectories involving C5 = C6 rotations increases first from 1 to 5 and then to 16. The shift toward isomerization of the terminal double bond is not linear with the distortion, but picks up momentum as the pre-twist angles increase. This is also evident from the data of model **4** in which the out-of-plane torsion is much closer to **3**, but the distribution is more similar to **2**. There is no clear pattern in the Z/E product ratio of C3 = C4 bond isomerization; in contrast the E product yield is very high throughout the model chromophores when the pre-twisted C5 = C6 bond isomerizes. These results are also summarized graphically in Fig. 7.

The sense of rotation of the isomerizing double bond is not relevant in the planar model **1**: both the clockwise and the counterclockwise rotation are equally probable. Within the limits set by the number of trajectories studied, this is borne out by the statistics of this chromophore. With the twist angles preset in a clockwise manner in the chromophores **2** to **4**, it is not surprising that the trajectories of C5 = C6 isomerization follow in the same direction without exception. Whether the preference for clockwise rotation about the (planar) C3 = C4 bond in these cases is significant or accidental cannot be decided on the basis of the available data.

With respect to the averaged data concerning the hopping event, there is a significant difference in the hopping geometries: for the C3 = C4 double bond most events take place between 120° and 110° of torsion, as observed already in the statistical analysis of **1**. Most of

the E/Z isomerizations of the terminal double bond happen between 75° and 85° of torsion, i.e., much closer to the product geometry. Also, in the latter case the average lifetime of the excited state is definitely shorter than for the central bond, possibly on account of the initial twist imparted on this bond. A report about how the reaction velocity is influenced by this effect has appeared recently [10].

Conclusions

The ultra fast, highly selective, and efficient photoisomerization of the retinal chromophore in the retinal binding proteins rho and bR has been probed on a small all-*E*-configurated 3-double-bond model chromophore using ab initio excited state MD methodology and employing a technique for analyzing the product distribution by following the motion of high-amplitude hydrogen-out-of-plane modes at possible decay events.

The following are our key findings:

- In the planar chromophore isomerization occurred almost exclusively at the central double bond with an overall yield of 60% of the *Z*-product; 40% of the trajectories returned to the initial *E*-configuration of the starting product. The average lifetime of the excited state was between 98 and 114 fs, depending on the method used for determining the surface-hopping event. For a trajectory to yield the *Z*-product, the S_1 to S_0 surface hopping should occur at the first close approach when the internal vibrational and rotational modes are still largely coupled. The probability for a return to the *E*-configuration increases with the number of unsuccessful close approaches, even though the continuous rotation of the double bond shifts the geometry of the molecule at the hopping event further toward the *Z*-product.
- Bond torsion significantly affects the product distribution of the model chromophores. With an initial torsion of the terminal bonds by 10° each, isomerization of the central double bond is still favored; 89% of the trajectories involve rotation of the C3 = C4 bond. However, 11% of the photoproduct show that isomerization has occurred at the C5 = C6 bond. Doubling the dihedral angles shifts the distribution further, to 63 and 37%, respectively. Whether the observed changes of the E/Z ratio are significant and can be correlated with observed quantum yields remains to be seen considering the limited number of trajectories available. The results show, however, convincingly that the initial torsion about certain bonds has a directing effect on the photochemistry of the chromophore.

The calculated isomer ratios, C3 = C4 versus C5 = C6, are far from the selectivity observed in real proteins. There are several factors that can contribute to this discrepancy. Our model chromophores are very short and cannot possibly reflect the whole complexity of a 6-double-bond chromophore. The preference for isomerizing the central double bond shown in model **1** would work very much in favor of the C11 = C12 bond in rho, in addition to it being *cis*-configurated and having a significant pre-twist. Larger models will have to be studied to come to a conclusive answer. Also, more work is needed to decide whether bond torsion can also be held accountable for the selective C13 = C14 bond isomerization in bR.

Acknowledgments This work was funded by the DFG Forschergruppe "Retinal Protein Action." We thank Dr. A.-N. Bondar and Dr. M. Sugihara for helpful discussion.

References

1. Mathies RA, Lugtenburg J (2000) The primary photoreaction of rhodopsin. In: Stavenga DG, DeGrip WJ, Pugh EN Jr (eds) Handbook of biological physics, vol 3. Elsevier, Amsterdam, pp 55–90
2. Okada T, Ernst OP, Palczewski K, Hofmann KP (2001) Trends Biochem Sci 26:318–324
3. Haupts U, Tittor J, Oesterhelt D (1999) Annu Rev Biophys Biomol Struct 28:367–399
4. Palczewski K, Kumasaka T, Hori T, Behnke CA, Motoshima H, Fox BA, Le Trong I, Teller DC, Okada T, Stenkamp RE, Yamamoto M, Miyano M (2000) Science 289:739–745
5. Okada T, Sugihara M, Bondar AN, Elstner M, Entel P, Buss V (2004) J Mol Biol 342:571–583
6. Luecke H, Schobert B, Richter HT, Cartailler JP, Lanyi JK (1999) J Mol Biol 291:899–911
7. Belrhali H, Nollert P, Royant A, Menzel C, Rosenbusch JP, Landau EM, Pebay-Peyroula E (1999) Structure 7:909–917
8. Vreven T, Bernardi F, Garavelli M, Olivucci M, Robb MA, Schlegel HB (1997) J Am Chem Soc 119:12687–12688
9. Garavelli M, Bernardi F, Olivucci M, Vreven T, Klein S, Celani P, Robb MA (1998) Faraday Discuss 110:51–70
10. Buss V, Weingart O, Sugihara M (2000) Angew Chem 39:2784–2786
11. Warshel A, Chu ZT (2001) J Phys Chem B 105:9857–9871
12. Ferré N, Olivucci M (2001) J Am Chem Soc 125:6868–6869
13. Andruniow T, Ferré N, Olivucci M (2004) Proc Natl Acad Sci USA 101:17908–17913
14. Freedman K, Becker RS (1986) J Am Chem Soc 108:1245–1251
15. Sugihara M, Buss V, Entel P, Hafner J, Bondar AN, Elstner M, Frauenheim T (2004) Phase Trans 77:31–45
16. Hayashi S, Tajkhorshid E, Schulten K (2002) Biophys J 83:1281–1297
17. Cembran A, Bernardi F, Olivucci M, Garavelli M (2004) J Am Chem Soc 126:16018–16037
18. Aharoni A, Hou B, Friedman N, Ottolenghi M, Rousso I, Ruhman S, Sheves M, Ye T, Zhong Q (2001) Biochemistry (Moscow) 66:1210–1219
19. Sugihara M, Buss V, Entel P, Elstner M, Frauenheim T (2002) Biochemistry 41:15259–15266
20. Frisch MJ, Trucks GW, Schlegel HB, Scuseria GE, Robb MA, Cheeseman JR, Zakrzewski VG, Montgomery JA, Stratmann RE, Burant JC, Dapprich S, Millam JM, Daniels AD, Kudin KN, Strain MC, Farkas O, Tomasi J, Barone V, Cossi M, Cammi R, Mennucci B, Pomelli C, Adamo C, Clifford S, Ochterski J, Petersson GA, Ayala PY, Cui Q, Morokuma K, Malick DK, Rabuck AD, Raghavachari K, Foresman JB, Cioslowski J, Ortiz JV, Baboul AG, Stefanov BB, Liu G, Liashenko A, Piskorz P, Komaromi I, Gomperts R, Martin RL, Fox DJ, Keith T, Al-Laham MA, Peng CY, Nanayakkara A, Challacombe M, Gill PMW, Johnson B, Chen W, Wong MW, Andres JL, Gonzalez C, Head-Gordon M, Replogle ES, Pople JA (1998) Gaussian 98, Revision A.9. Gaussian Inc., Pittsburgh

21. Terstegen F, Carter EA, Buss V (1999) Int J Quantum Chem 75:141–145
22. Andersson K, Barysz M, Bernhardsson A, Blomberg MRA, Cooper DL, Fülscher MP, de Graaf C, Hess BA, Karlström G, Lindh R, Malmqvist PÅ, Nakajima T, Neogrády P, Olsen J, Roos BO, Schimmelpfennig B, Schütz M, Seijo L, Serrano-Andrés L, Siegbahn PEM, Stålring J, Thorsteinsson T, Veryazov V, Widmark PO (2002) MOLCAS Version 5.4. Lund University, Sweden
23. Fox DJ, Osamura Y, Hoffmann MR, Gaw JF, Fitzgerald G, Yamaguchi Y, Schaefer HF (1983) Chem Phys Lett 102:17–19
24. Sloane CS, Hase WL (1977) J Chem Phys 66:1523–1533
25. Tully JC, Preston RK (1971) J Chem Phys 55:562–572
26. Paterson MJ, Hunt PA, Robb MA, Takahashi O (2003) J Phys Chem A 106:10494–10504
27. Groenhof G, Bouxin-Cademartory M, Hess B, De Visser SP, Berendsen HJC, Olivucci M, Mark AE, Robb MA (2004) J Am Chem Soc 126:4228–4233
28. Weingart O, Migani A, Olivucci M, Robb MA, Buss V, Hunt P (2004) J Phys Chem A 108:4685–4693
29. Weingart O, Buss V, Robb MA (2005) Phase Trans 78:17–24